Colloid Polym Sci 276:219–231 (1998)

ORIGINAL CONTRIBUTION

D. Duracher
F. Sauzedde
A. Elaissari
A. Perrin
C. Pichot

Cationic amino-containing *N*-isopropylacrylamide–styrene copolymer latex particles: 1-Particle size and morphology vs. polymerization process

Received: 21 August 1997
Accepted: 22 October 1997

D. Duracher · F. Sauzedde · A. Elaissari
A. Perrin · C. Pichot (✉)
Ecole Normale Supérieure de Lyon
CNRS-bioMerieux
46 allée d'Italie
69364 Lyon
France
E-mail: Christian.Pichot@ens-bma.cnrs.fr

Abstract Cationic hydrophilic copolymer latexes were synthesized at 70 °C either by batch or two-step emulsifier-free emulsion polymerization of styrene (St), *N*-isopropylacrylamide (NIPAM), and aminoethylmethacrylate hydrochloride (AEM) using 2,2′-azobis (2-amidinopropane) dihydrochloride as initiator. At first, batch polymerization kinetics were followed by gas chromatography (GC), revealing that NIPAM rapidly homopolymerized, before the polymerization of styrene had started. Particle size analysis by quasi-elastic light scattering (QELS) and transmission electron microscopy (TEM) showed that monodispersed particles were obtained with the formation of a poly[NIPAM] rich shell. Adding a small amount of the cationic monomer caused a strong decrease of the particle size without affecting the size monodispersity. When a shot process was used, a narrow particle size distribution was maintained, provided that the monomer addition was performed at a relatively high conversion of the first batch step. The poly[NIPAM] rich shell layer was larger with the shot process, but increasing the amino-containing monomer in the recipe resulted in a dramatic decrease of the thickness. Combination of transmission, scanning and atomic force microscopy techniques showed that these hydrophilic particles exhibited odd-shaped structures, the unevenness being dependent upon the performed process. Kinetic data and particle morphology information were inferred for discussion of the polymerization mechanism of this system.

Key words Emulsion polymerization – styrene, *N*-isopropylacrylamide – cationic monomer – batch and shot process – particle size and morphology

Introduction

In the past decade, increasing attention has been paid to the preparation and characterization of thermally sensitive polymer particles which were found to offer unique properties for many applications, especially in the biological field [1, 2]. The drastic change in the hydrophilic–hydrophobic character of the polymer for a given temperature (the so-called lowest critical solubility temperature (LCST)) results in a corresponding large variation of the colloidal properties of the particles (especially their particle size, electrophoretic mobility, colloidal stability, etc.) [3–6]. Hence, such particles exhibit outstanding capabilities for the immobilization and release of biologically-active molecules [7, 8].

Previous works devoted to the preparation of thermosensitive particles was pioneered both by Pelton in the

case of poly[*N*-isopropylacrylamide] either alone [3] or with styrene [6] and by Kawaguchi and coworkers [9–12] in the case of the emulsifier-free emulsion copolymerization of styrene with various *N*-substituted-acrylamide derivatives. Polymerization of NIPAM in the aqueous phase was clearly shown to proceed via a precipitation polymerization mechanism [13, 14] provided the reaction temperature was performed above the LCST of the polymer (ca 32 °C) and in the presence of a cross-linking monomer. Due to the huge propagation rate constant, k_p of acrylamide derivatives, polymerization occurred very rapidly and led to the production of monodisperse hydrogel particles in the submicron size range exhibiting the above-mentioned properties vs. temperature. In the case of the copolymerization of styrene with *N*-substituted acrylamides, the polymerization mechanism has been experimentally explored and discussed by Kawaguchi et al. [12, 15]. Polymerization of the hydrophilic monomer in the aqueous phase was shown to be the first event, leading to the production of a large number of small particles into which the hydrophobic monomer could diffuse and polymerize. The morphology of the particles was found to reflect this two-step polymerization mechanism, unevenly shaped particles being in evidence as a result of a phase-demixing process between the early formed polymer and the rich-styrene polymer later produced inside the particles. The extent of phase separation has been investigated as a function of conversion, nature and molar ratio of the *N*-substituted acrylamide.

As a part of a research program to prepare well-characterized thermosensitive and reactive particles suitable for the covalent immobilization of biologically active macromolecules, the objective of this paper is to report on the synthesis of cationic amino-containing *N*-isopropylacrylamide-styrene copolymer particles. A preliminary kinetic study is performed on the batch reaction polymerization between styrene and NIPAM whether a cationic monomer, the aminoethylmethacrylate, hydrochloride (AEM) is used or not. Then, latex particles are produced upon varying the AEM content by a shot-growth process. Particle size and morphology of the different latexes vs. conversion were examined using various techniques, allowing to get further insights on the polymerization mechanism involved.

Experimental

Materials

Styrene monomer (99% pure from Janssen) was purifed by vacuum distillation and stored at −20 °C. *N*-isopropylacrylamide (NIPAM) (from Kodak) was purified using a 60/40 (v/v) of hexane and toluene mixtures. Methylene bisacrylamide (MBA) (from Aldrich) was used as cross-linking monomer and 2-aminoethylmethacrylate hydrochloride (AEM) (from Kodak) was used as the functional monomer. These two monomers were used as received. 2,2′-azobis (2-amidinopropane) dihydrochloride (V50) (from Wako) was used as the cationic initiator; it was recrystallized from 50/50 (v/v) acetone/water mixture, dried under vacuum. Well-deionized and deoxygenated water was used in all synthesis.

Synthesis of latexes

Poly(styrene/*N*-isopropylacrylamide) P(St/NIPAM) and poly(styrene/*N*-isopropylacrylamide/aminoethylmethacrylate) P(St/NIPAM/AEM) latexes were synthesized under emulsifier-free emulsion polymerization. All polymerizations were carried out in a 250 ml four-neck glass reactor flask equipped with a glass anchor-type agitator (200 rpm), condenser and nitrogen inlet. The reaction temperature was controlled at 70 °C.

Preparation of P(St/NIPAM/AEM) batch latex particles

The polymerization was performed under emulsifier-free emulsion polymerization using styrene, NIPAM, AEM and V50 as initiator. The final conversion was gravimetrically determined. The recipe established by Makino et al. [5] for anionic latex particles was modified so as to prepare cationic latex particles in a size range of 400 nm and bearing a hydrophilic shell layer. The recipe is given in Table 1 (for PSt, DD1A, DD1B and DD2). Polystyrene latex particles (PSt) was prepared by batch polymerization using the same recipe, as described above, without NIPAM and AEM monomer.

Table 1 Latex recipe for batch process (for PSt, DD1A, DD1B and DD2 samples)

Reagents	PSt	DD1A and DD1B	DD2
Water[g]	200	200	200
Styrene [g]	18	18	18
NIPAM [g]	0	2	2
AEM [g]	0	0	0.06
V50 [g] (Initiator)	0.2	0.2	0.2

Table 2 Latex recipe for shot process (DD3–DD12 samples)

Reagents	DD3–DD9	DD10	DD11	DD12
Batch latex particles at a given conversion				
Water [g]	25	25	25	25
NIPAM [g]	5.07	5.07	5.07	5.07
AEM [g]	0.147	0	0.220	0.294
MBA [g]	0.069	0.069	0.069	0.069
V50 [g]	0.122	0.122	0.122	0.122

Preparation of P(St/NIPAM/AEM) core-shell latex particles

These latexes were produced by adding NIPAM, MBA, AEM and the initiator (V50) after a batch styrene–NIPAM emulsion copolymerization was started. Shot additions were carried out at different reaction times with a varying amount of AEM. Table 2 shows the general recipe used for this synthesis (for run DD3 to DD12).

Conversion

The overall conversion was gravimetrically determined during the polymerization. The material balance between particles and aqueous phase gave the water-soluble polymer content. The consumption of NIPAM and styrene were analyzed by gas chromatography (9000 Perkin–Elmer). The column phase was a 10% carbowax 20 M onto chromosorb WAW 80 400; detection was performed with a flame ionization detector (oven temperature 200 °C, detector and injector temperature 250 °C).

Partition of monomers

Partition of *N*-isopropylacrylamide between styrene and the water phase (at 70 °C and in concentrations similar to that carried out for the latex synthesis) was measured by ^{1}H NMR spectroscopy (Bruker AC 200) in deuterated methanol using trimethyl silyl-3 propionic acid (TMS) as an external standard.

Particles size analysis

The hydrodynamic size of latex particles was determined by quasi-elastic light scattering using a Coulter N4 (Coultronics) submicrometer particle size analyser. Transmission electron microscopy of the latex particles was carried out using a Philips CM120 microscope (Centre de Microscopie Electronique Appliquée à la Biologie et al. Géologie (CMEABG) at Claude Bernard University, Lyon I, France). The particle size of dry latex and its distribution were determined by the size measurement of more than 50 particles on a Helwett Packard 911 A digitalyser.

Atomic force microscopy (AFM) and scanning electronic microscopy

AFM was carried out on an Autoprobe Cp instrument (Park Scientific Instrument, Sunnyvale), using a non-contact mode. The shape of the particles was observed by SEM (Hitachi S 800, CMEABG at Claude Bernard University, Lyon I, France). Samples for SEM and AFM were prepared by placing a drop of the dispersion directly onto an aluminium sample holder (or silicon oxide wafers for AFM) and drying the latex at room temperature. All specimens for SEM measurements were sputtered with gold at fixed conditions (time 150 s, current 20 mA, voltage 2 kV). A standard voltage (10 kV) was used for SEM experiments.

Results and discussion

The preparation of hydrophilic and temperature-sensitive latex particles bearing amino groups in a protected form was performed by using styrene to construct the particle core and a *N*-isopropylacrylamide/2-aminoethylmethacrylate mixture to form the shell (which was cross linked upon addition of methylene bisacrylamide). A kinetic study was first investigated on the batch emulsion copolymerization of the styrene–NIPAM monomer mixture whether AEM was added or not, followed by shot-growth polymerization.

Synthesis of P(St/NIPAM) and P(St/NIPAM/AEM) batch latexes

Conversion vs. time curves of P(St/NIPAM) (DD1A) and P(St/NIPAM/AEM) (DD2) batch emulsifier-free emulsion copolymerizations are reported in Fig. 1 together with that of styrene (PSt) homopolymerization for comparison. For reproducibility purposes, the former experiment was carried out twice (DD1B). As expected, the addition of hydrophilic monomers results in a strong increase of the polymerization rate as well as a rise in the final conversion. It requires 5 h to get a plateau conversion for styrene–NIPAM copolymerizations instead of 7 h for

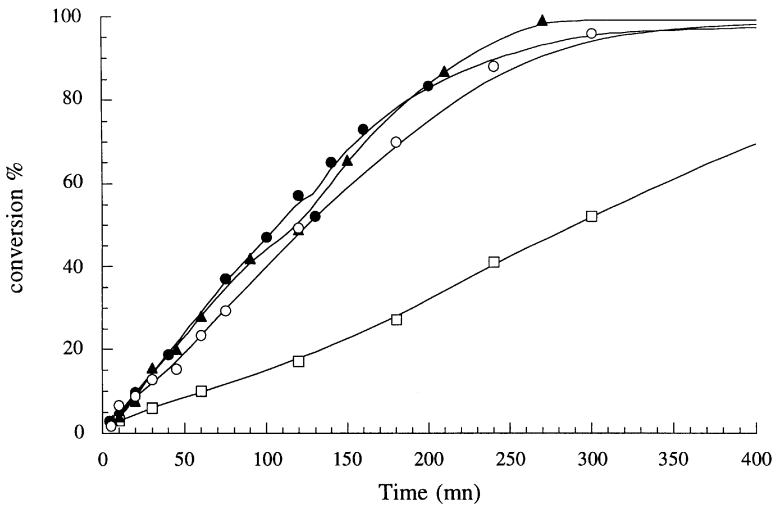

Fig. 1 Conversion vs. time curves of emulsifier-free emulsion (co)polymerization of styrene and NIPAM with and without AEM: (—□—) batch without NIPAM (PSt); (—○—) batch with NIPAM (DD1A & B); (—▲—) batch with NIPAM and AEM (DD2); (—●—) shot with NIPAM and AEM (DD3-12)

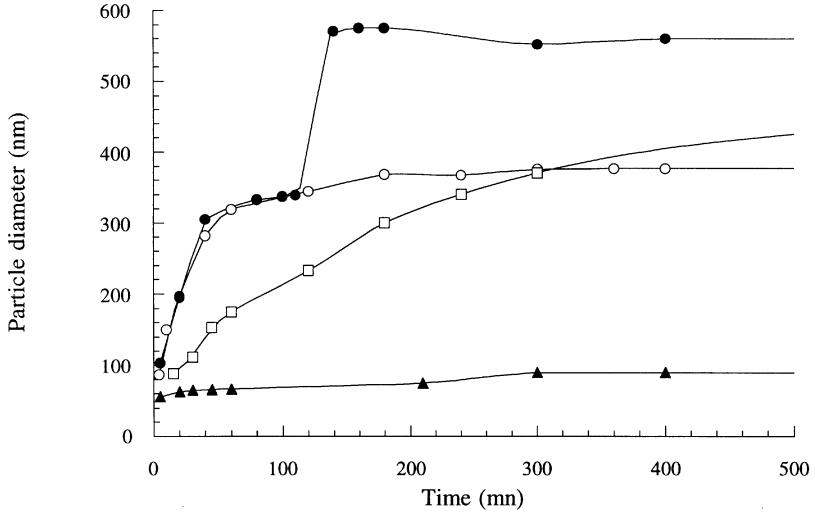

Fig. 2 Particle size vs. time for batch and shot-growth emulsion copolymerization of styrene and NIPAM. (Effect of adding AEM): (—□—) batch without NIPAM (PSt); (—○—) batch with NIPAM (DD1A & B); (—▲—) batch with NIPAM and AEM (DD2); (—●—) shot with NIPAM and AEM (DD3-12)

styrene homopolymerization. In the first case, this conversion is almost completed (95%) but is only around 80% in the latter case. Adding the cationic monomer (AEM) (DD2) slightly increases the polymerization rate and conversion yield (97%). Such a kinetic behavior is well known and was extensively discussed by many authors performing emulsion polymerization of styrene in the presence of ionic or water-soluble hydrosoluble monomers [15]. The large increase in the polymerization rate is generally attributed to the influence of the functional monomer which dramatically affects the early step of the nucleation period; a huge number of precursor particles are formed which rapidly suffer a limited coagulation period providing mature particles. This mechanism is considered to take place in this system as well as with similar non-ionic monomers [15, 16].

Particle size and distribution of the various latexes were measured both by quasi-elastic light scattering (at 20 °C and 50 °C, respectively) and transmission electron microscopy. Particle diameter (as obtained by QELS at 20 °C) vs. time is plotted in Fig. 2, and final particle sizes are given in Table 3. It is worth mentioning that particle size reaches a pseudoplateau much more rapidly for polymerization carried out in the presence of NIPAM and NIPAM/AEM mixture. For these latexes, particle diameters of 345 and 80 nm, respectively, are attained within a few minutes whereas it requires a much longer time for styrene homopolymerization. As illustrated in Table 3, QELS particle diameter of DD1A and DD1B final latexes are larger at room temperature than at 50 °C (i.e. above the LCST of the poly[NIPAM]), reflecting the presence of the expanded hydrophilic layer around the particles. In the

Table 3 Batch emulsifier-free emulsion copolymerization of styrene with NIPAM and AEM

Sample	Conversion [wt%]	Particle size and distribution			PDI[a)]	Water soluble polymer [wt%]
		D_h 20 °C [nm]	D_h 50 °C [nm]	D_{MET} [nm]		
PSt	83	420	420	414	1.021	1.5
DD1A	95.2	356	310	306	1.007	1.3
DD1B	94	376	330	326	1.017	1.2
DD2	96.4	85	*	78	b)	*

* Not measured due to the difficulty in centrifuging these low size particles.
a) Polydipersity of latex particles.
b) Fairly monodisperse.

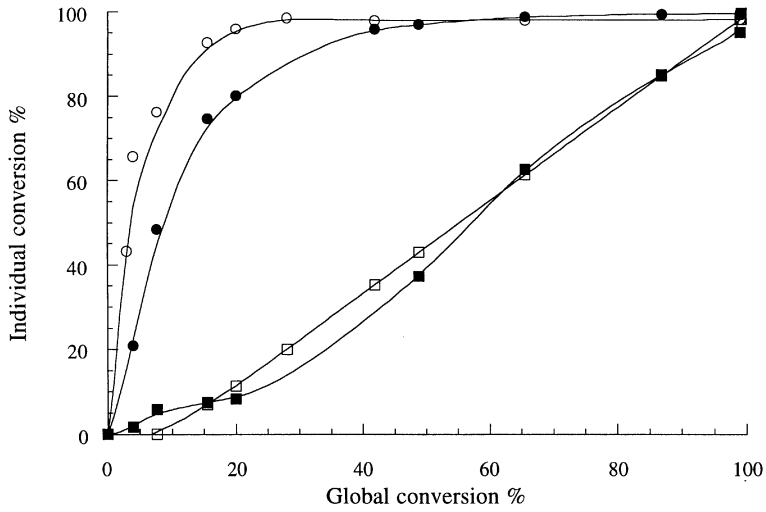

Fig. 3 Individual conversion vs. overall conversion for batch emulsion copolymerization of styrene and NIPAM with and without AEM: (—■—) styrene without AEM (DD1A); (—●—) NIPAM without AEM (DD1A); (—□—) styrene with AEM (DD2); (—○—) NIPAM with AEM (DD2)

case of DD2 sample, due to the smaller size, the discrepancy is less obvious. Except for polystyrene latex, the particle sizes measured by TEM are slightly underestimated due to the shrinkage of the water-swollen particles under the electron beam. The particles appear quite monodisperse in their dried and shrunk state. It should be remembered, as claimed for such microgel particles, that even at 50 °C, particles woud contain of the order of 10–20 wt% of water [17–19], which could explain the lower size obtained by TEM. Finally, the amount of water-soluble species (mostly oligomers) is not significant (order of 1.5 wt%), which is indicative that poly[NIPAM] is strongly entangled within the particles.

More information was obtained on the batch polymerization by following the individual monomer conversion vs. time of styrene and NIPAM by gas chromatography as illustrated in Fig. 3. It is clearly shown that most of NIPAM is entirely consumed (80%) before styrene starts to polymerize. The effect is even more pronounced when AEM was added in the initial monomer mixture since conversion of NIPAM is almost completed after 20% of overall conversion. Two main factors may contribute to this kinetic behavior: (i) the water solubility of NIPAM and (ii) the huge absolute propagation rate constant k_p for this monomer compared to that of styrene.

The evolution of the particle size and distribution was also examined by TEM as a function of the conversion. The TEM micrographs of various latex samples withdrawn at increasing conversion of a styrene–NIPAM batch emulsion polymerization are given in Fig. 4. The corresponding particle size variation vs. conversion as measured by QELS (20 °C) and by TEM are reported in Table 4.

At very low conversion (2%), a mixture of very tiny and numerous particles is clearly observed in the size range 2–20 nm; they are supposed to contain mostly collapsed poly[NIPAM] chains. As polymerization proceeds (at ca 10% conversion), the particle size increases (order of

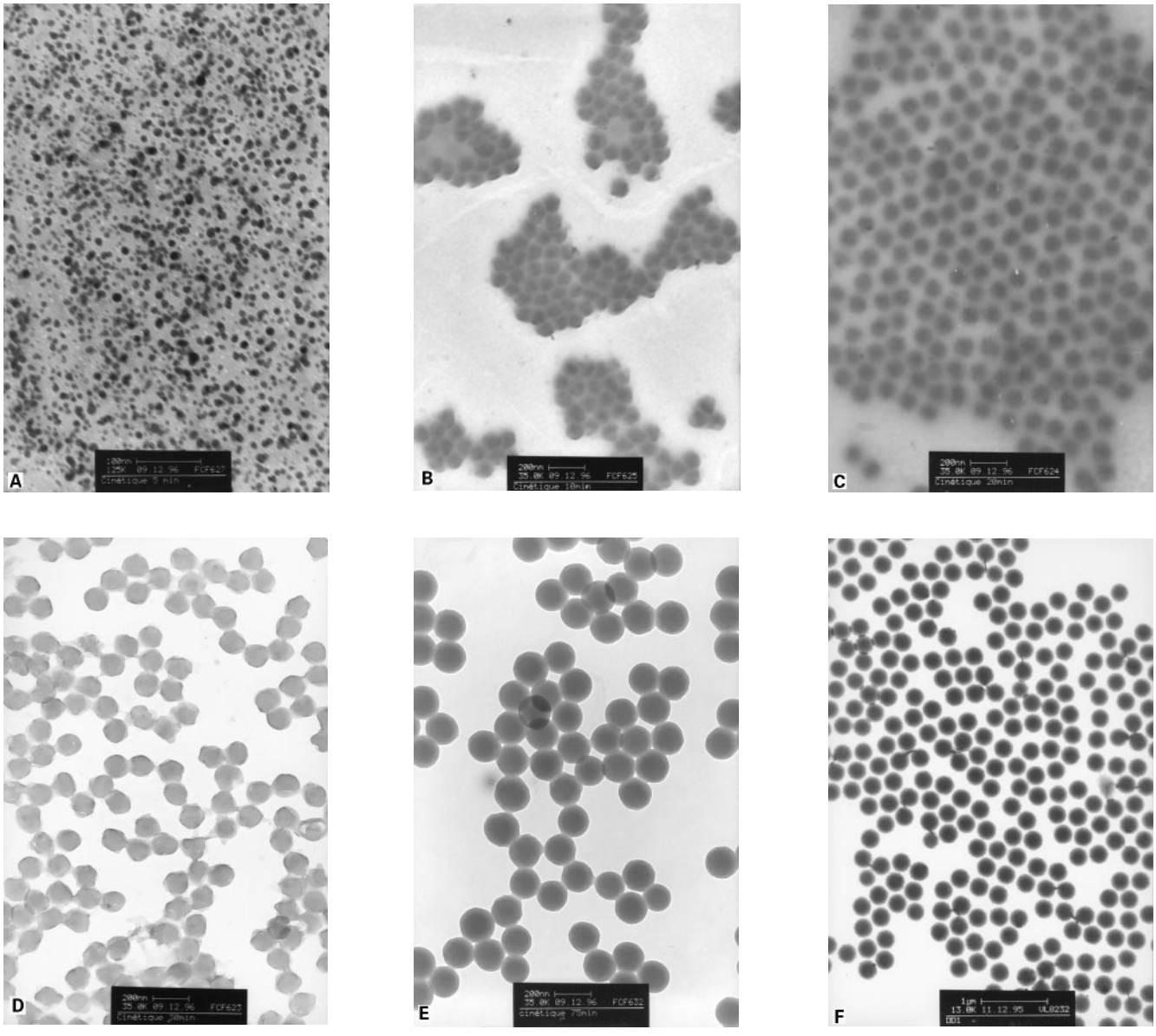

Fig. 4 Electron micrographs (TEM) of latexes as a function of conversion for batch emulsion copolymerization of styrene–NIPAM (sample DD1A): (A) 2% conversion; (B) 7% conversion; (C) 10% conversion; (D) 14% conversion; (E) 30% conversion; (F) 95% conversion

70 nm) and the size distribution becomes narrow (1.007) which could suggest that small particles formed early have grown through a limited flocculation step. It is interesting to note that TEM and QELS particle diameters already strongly differ, a confirmation of the hydrophilic character of the formed particles (at room temperature). Above this conversion, the particles continue to grow and simultaneously their particle shape appears more clearly delineated; however, at 14% conversion, the particle exhibits an uneven structure which progressively disappears at higher conversion. From the kinetics, this conversion corresponds to the onset of styrene polymerization, therefore poly[NIPAM]-rich particles, which exhibit a hydrophobic character at the reaction temperature can be swollen with styrene. As polymerization proceeds, the particle size increases with always a largest diameter for QELS data, however, the size difference is decreasing since only styrene polymerizes within the particles. Moreover, the darkness of the particles appears more marked upon increasing conversion, which also indicates that polystyrene

Table 4 Particle size variation vs. conversion in styrene–NIPAM emulsifier-free emulsion copolymerization (DD1A experiment)

Conversion [%]	Particle size [nm]	
	TEM	QELS
2	2–20	*
7	70	140
9	91	166
15	145	193
23	172	200
30	200	220
49	*	270
70	*	287
96	316	345

* Not determined.

progressively plays a predominant part in the particles. All these observations seem to corroborate a two-steps polymerization mechanism for this system.

Synthesis of P(St/NIPAM) and P(St/NIPAM/AEM) shot latexes

Based on this preliminary kinetic study, a shot-growth process was performed so as to favor the surface incorporation of the cationic amino-containing monomer (AEM) and to control the thickness of the shell layer. As detailed in the experimental section, the influence of two main factors was examined: (i) the addition of the NIPAM–MBA–AEM mixture at different conversions of an emulsifier-free polymerization of styrene/*N*-isopropylacrylamide; (ii) the variation of the content of AEM monomer with a view to increasing the amino surface charge density. Kinetic data were expressed in terms of conversion, particle size and amount of formed water-soluble polymers as compiled in Table 5. At first, as illustrated in Fig. 1, the conversion vs. time curves for experiment DD3 (where the shot monomer addition was carried out at 57% conversion) are very similar to that of the corresponding styrene–NIPAM batch polymerization. On the contrary, as shown in Fig. 2, there is a large size increase (ca around 200 nm) of the final shot latex particles, which suggests that this process drastically enhances the shell thickness.

Let us now consider the influence of the conversion of the seed at which the shot addition is performed. It appears that a polydisperse latex is formed (Table 5 and Fig. 7(a)) when this conversion is too low, i.e. below 50% (DD7 sample). Except under these conditions, there is no significant effect on the final particle size of the shot latexes whether the measurement was performed by QELS (20 °C or 50 °C) or by electron microscopy. With this last method, the particle diameter is again lower than the QELS size data in 50 °C. The amount of water-soluble polymers is larger than in batch polymerization (in between 15 and 18 wt% of the total polymer material).

As regards to the influence of the AEM concentration in the monomer mixture added in the second step, and carried out at similar conversion (around 70%), two main results can be pointed out: (i) a decrease in the particle size as measured by QELS at room temperature, i.e. when the hydrophilic shell layer is expanded (below the LCST); (ii) the amount of hydrosoluble species strongly increases upon increasing the AEM concentration. The first effect can be interpreted by the chain transfer activity of the amino-containing monomer (AEM) (even under protected form) in radical polymerization as recently shown in the emulsion polymerization of styrene in the presence of this cationic monomer [20]. A huge transfer rate constant was, indeed, determined (around $10\,l\,mol^{-1}\,s^{-1}$) suggesting that this transfer would also occur in the case of NIPAM polymerization. That would cause a decrease of the average chain length of the copolymer incorporated at the surface of the core latex. Cross-linking density (due to MBA) would be concomitantly reduced, making unfavorable a tight entanglement of the polymer chains in the shell layer upon increasing the AEM content. As illustrated in Fig. 5, such a transfer reaction results in the formation of a more and more thinner shell upon increasing the AEM concentration. This effect is very slightly reflected when particle sizes are measured by QELS at 50 °C and not at all by TEM measurements since the shell layer is fully collapsed at this temperature in the dried and shrunk state. The increasing amount of the water-soluble polymers is also a consequence of the presence of AEM in the latex recipe. First, due to a copolymerization effect (reactivity parameters of methacrylate monomers are larger than that of acrylamide derivatives in corresponding binary systems) [21], rich-AEM copolymers formed at the beginning exhibit a polyelectrolyte character having a LCST presumably above that of pure poly[NIPAM]. Secondly, as already suggested, due to the transfer reaction, there is a decrease in the number-average chain length and the production of low molecular weight polymers and oligomers which are left in the aqueous phase.

Further studies on particle surface morphology of the batch and shot latexes

Complementary analysis of the latex particles was performed in order to get more details on the particle surface morphology as a function of the polymerization process.

Table 5 Shot-growth emulsion copolymerizations of styrene with NIPAM and AEM

Sample no.	AEM [%]	Conversion [wt%]		Particle size			PDI[a)]	Water soluble polymer [wt%]
		[shot %]	[final %]	D_h 20 °C [nm]	D_h 50 °C [nm]	D_{MET} [nm]		
DD7	2	31	81.6	*	*	*	1.7	—
DD3	2	57	80.0	573	325	321	1.046	17.5
DD9	2	79	78.3	460	343	303	1.009	18.7
DD8	2	87	83.2	453	352	324	1.009	13.0
DD4	2	89	79.3	551	358	303	1.011	15.8
DD5	2	94	83.3	595	385	315	1.010	16.1
DD6	2	97	82.6	580	364	335	1.008	15.8
DD10	0	70	73.2	603	364	288	1.012	13.1
DD12	3	70	69.2	484	334	302	1.004	29.8
DD11	4	70	75.2	358	315	303	1.005	20.4

[a)] Polydispersity of latex particles.
* Polydisperse latex.

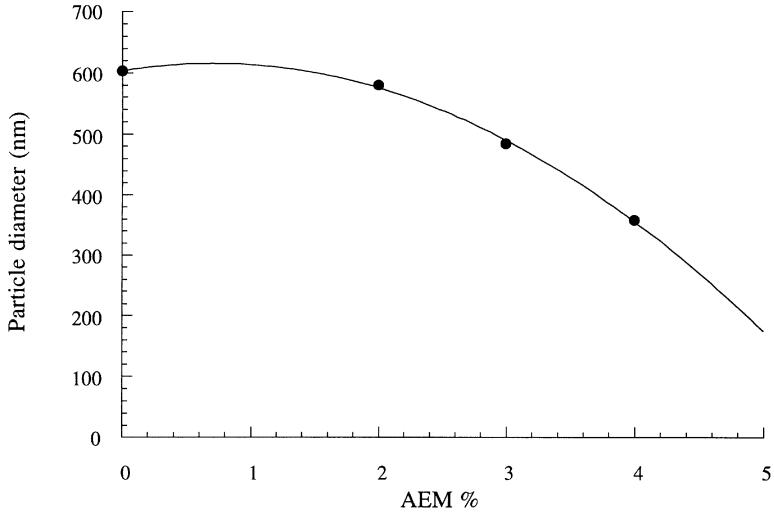

Fig. 5 Variation of particle size for shot-growth P(St–NIPAM–AEM) latexes as a function of molar percent of AEM/NIPAM introduced in the shot growth

At first, AFM in non contact mode was used so as to compare the particle morphology of three different styrene–NIPAM copolymer latexes and that of a polystyrene latex, as illustrated in Fig. 6. As expected, polystyrene particles (PSt sample) appear quite smooth, whereas P(St/NIPAM) batch (DD1A) and core-shell copolymer particles (DD3) exhibit a raspberry-like structure, the surface heterogeneity being better defined in the latter sample. For the DD2 latex prepared in the presence of the cationic monomer, no apparent structuring can be observed, due to the small size of the latex and the resolution limit of the AFM technique.

For DD1A and DD3 samples, the shell layer seems to be constituted of small spherical patches of relatively regular size (30–60 nm). As already stated, it is thought that the surface roughness in P[St/NIPAM] particles reflects the polymerization mechanism which occurs and results in the formation of a rich-poly[NIPAM] shell in both types of particles. When dispersed in water at room temperature (i.e. below the LCST), the rich-poly[NIPAM] chains are fully expanded as evidenced by QELS whereas after drying, they collapse on the highly rigid polystyrene-rich core. The roughness difference between the batch and shot particles may indicate how the hydrophilic monomer had polymerized early in the former process and at a later stage in the latter one.

Much information was deduced from scanning electron microscopy as illustrated in Figs. 7 and 8 for batch and shot latexes, respectively. At first, the above observed structures are qualitatively corroborated according to the

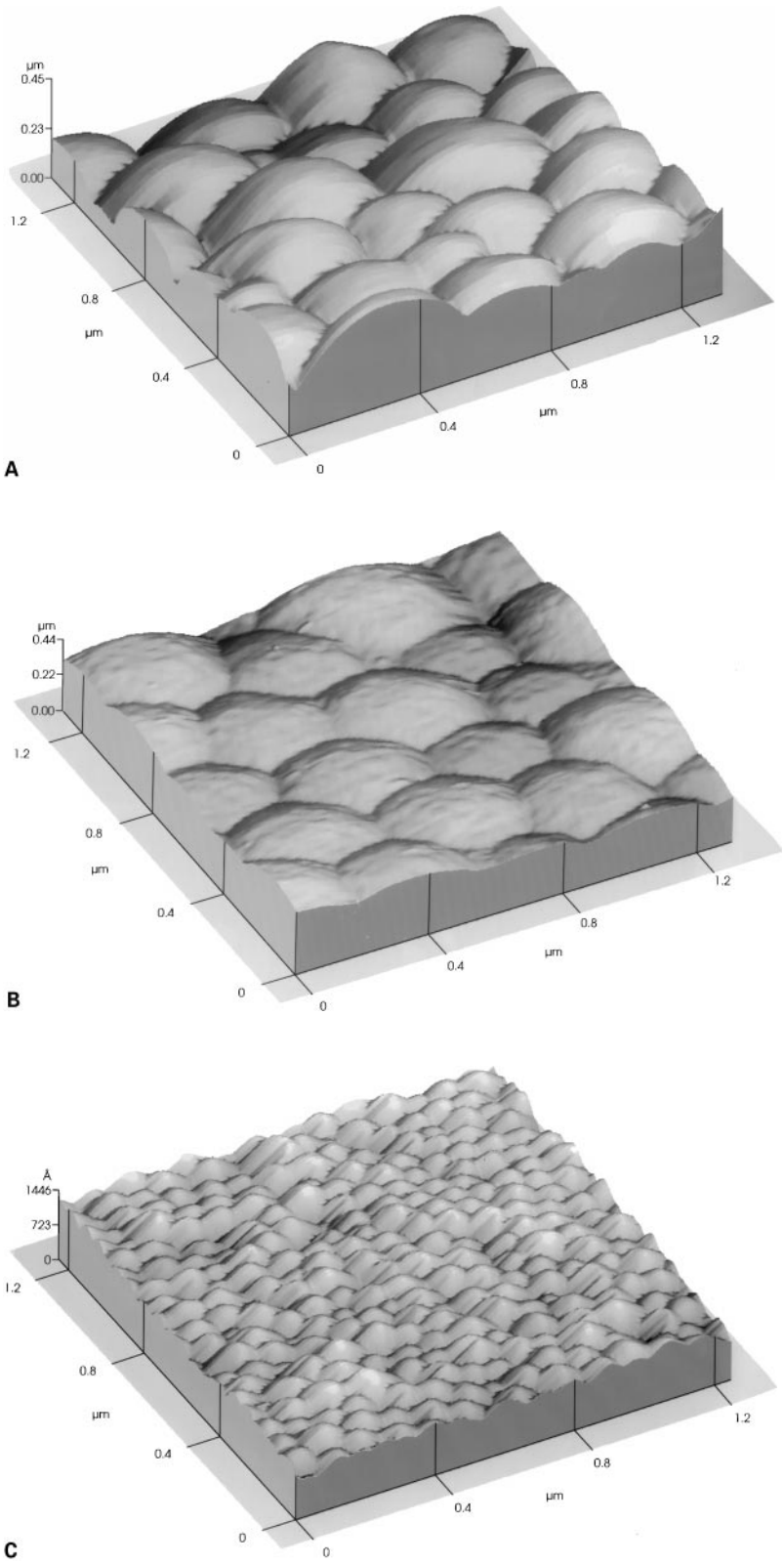

Fig. 6 AFM images of latex particles at end of conversion: (A) polystyrene latex (PSt); (B) batch P(St–NIPAM) without AEM (DD1A); (C) batch P(St–NIPAM) with AEM (DD2); (D) shot-growth P(St–NIPAM–AEM) (DD3)

Fig. 6 (Continued)

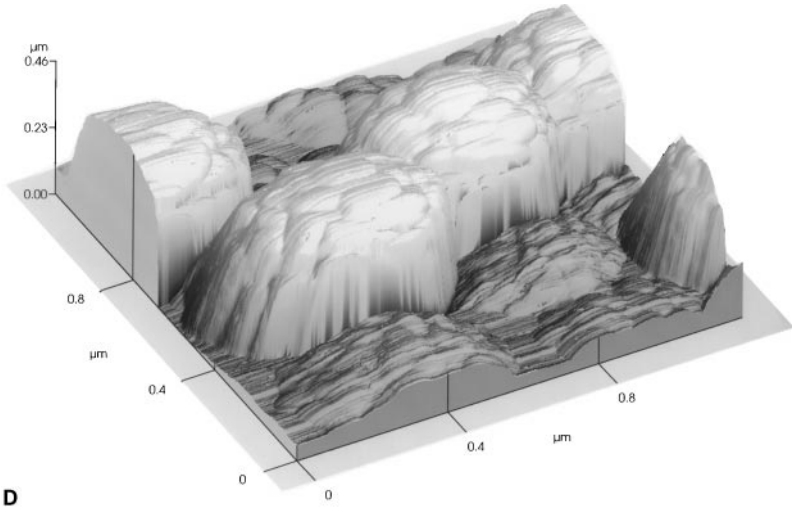

type of process (batch vs. shot growth), but with a better resolution due to the sample preparation. Batch styrene–NIPAM copolymer particles exhibit a slight roughness with small asperities still appearing (size domain order of 10–20 nm). For those prepared in the presence of the cationic monomer (but with a lower size, ca 80 nm), an uneven structure is revealed (which could not be observed by AFM). In the case of shot latexes (Fig. 7), it is clearly evidenced that the odd-shaped structure is dependent upon the conversion at which the shot addition of NIPAM was performed. The size domain of the small asperities is of the same order as that previously observed by AFM. The surface roughness appears more clearly when the shot addition of the monomer mixture occurred at low conversion (30% and 57% for DD3 and DD7 samples, respectively) whereas the particle surface is becoming smoother when this shot addition takes place at higher conversion (89% and 97% in DD4 and DD6 sample). It is interesting to mention that the same smooth particle shape was observed both by AFM and SEM techniques. This reflects the complexity of the polymerization mechanism when dealing with a shot process as will be discussed below.

Discussion and conclusion

Emulsifier-free emulsion copolymerization of styrene in the presence of NIPAM and a cationic amino-containing monomer has been performed with a view to preparing monodisperse submicron particles bearing reactive groups suitable for further investigating covalent immobilization of biomolecules. Due to the physicochemical properties of NIPAM and AEM water-soluble monomers, the polymerization behavior of this heterogeneous system was dramatically affected, which was reflected both by the observed variations in the particle size and surface morphology of the latexes. The above described results appear quite instructive for further discussing some features of the polymerization mechanism of this complex system whether a batch or a shot process is carried out.

First, concerning the batch process as already proposed by Kawaguchi et al. for other similar monomers [10, 15], it is clear that a two-step mechanism takes place as follows:

(i) At the very beginning, because of its favorable partitioning in the aqueous phase (around 60 wt% under experimental conditions), NIPAM rapidly reacts (with may be some solubilized styrene molecules (0.3 g/l water)), leading to polymer chains which precipitate at very low conversion (ca order of 2%), as tiny precursors; then these small and poorly stable nuclei coagulate, producing larger particles (order of 50–90 nm) with already a narrow size distribution (even at 10% conversion). According to GC kinetics, only a few percent of the initial styrene concentration is involved in this preliminary step, a further indication that NIPAM polymerizes more readily than acrylamide in such systems [15]. QELS diameters of these particles and their variation vs. temperature confirm that they are mostly composed of poly[NIPAM] chains.

(ii) At 20% conversion, more than 80% of the NIPAM has already polymerized, whereas styrene starts to react due to the diffusion of the monomer from the droplets and the subsequent swelling of the hydrophobic poly[NIPAM]-rich particles. Polystyrene chains are

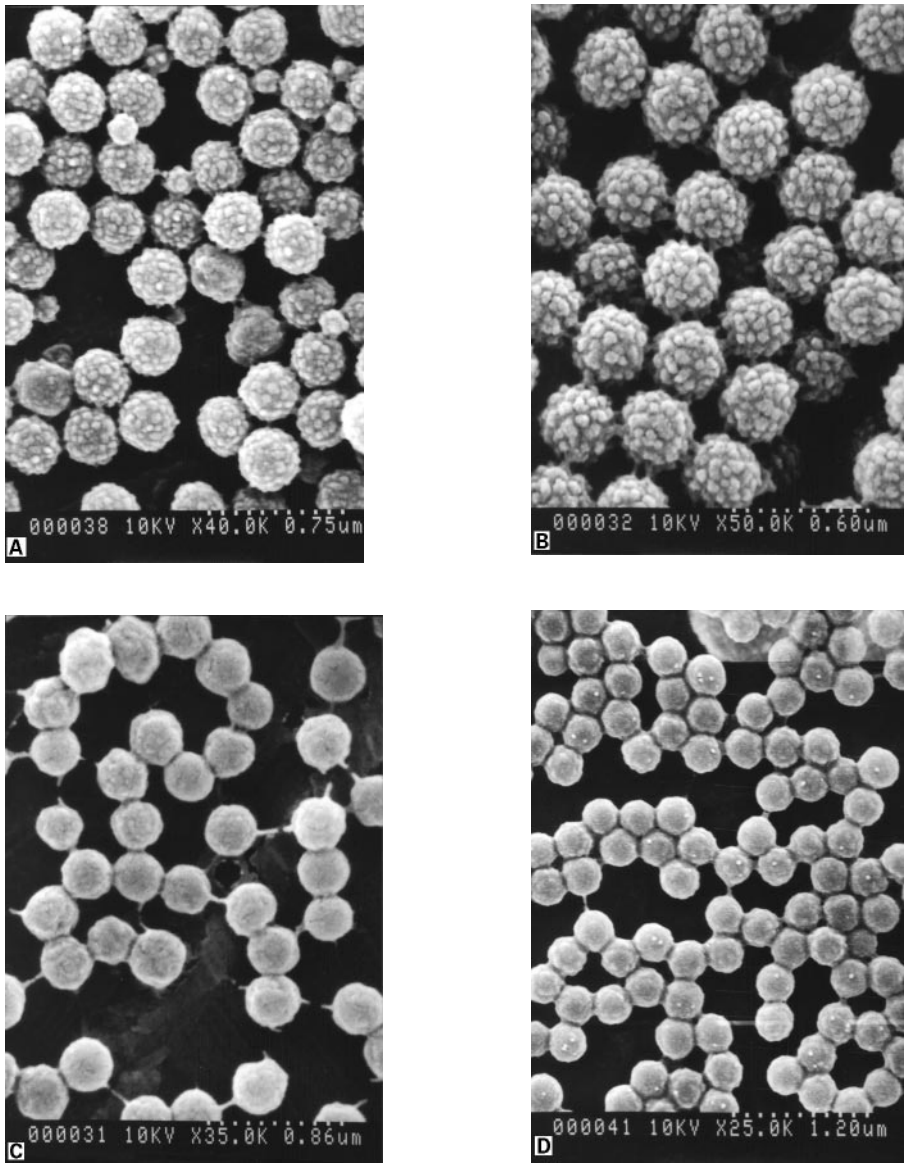

Fig. 7 Scanning electron micrograph of shot-growth P(St–NIPAM–AEM) latexes as a function of batch conversion: (A) DD7 shot at 31% conversion; (B) DD3 shot at 57% conversion; (C) DD4 shot at 89% conversion; (D) DD6 shot at 97% conversion

formed inside these particles, but due to a poor compatibility with the already formed poly[NIPAM], a phase separation rapidly occurs leading to some change in the initial particle morphology and formation of small polystyrene-rich occlusions.

(iii) As polymerization proceeds, the polystyrene phase becomes predominant, expelling most of the poly[NIPAM] at the particle surface. It should be reminded that a similar particle structure has been postulated in the case of the emulsifier-free copolymerization of styrene and acryloyl piperidine, a hydrophilic monomer having the same physicochemical properties as NIPAM [11]. However, a careful examination of the particle surface morphology in the final latexes (namely either by SEM or AFM techniques), showed small asperities. This corroborates the presence of polystyrene-rich occlusions which have demixed during polymerization and which have been covered later on by a thin layer of poly[NIPAM] chains.

Adding a small amount of AEM in the initial comonomer mixture leads to a change in the polymerization mechanism. At first, due to the exclusive partitioning of this water-soluble monomer in the aqueous phase and a copolymerization effect in favor of AEM (methacrylates derivatives are usually more reactive than acrylamide ones in binary copolymerization), the overall polymerization

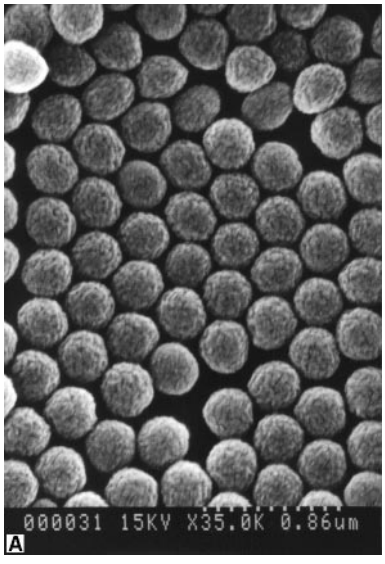

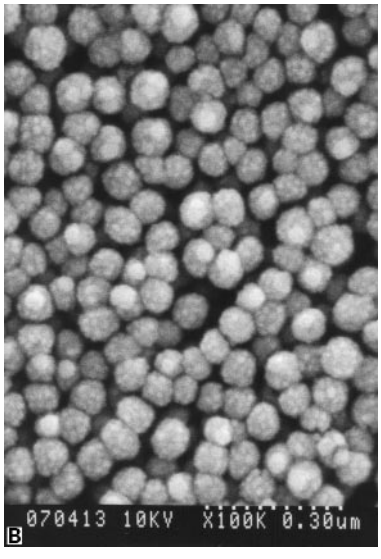

Fig. 8 Scanning electron micrographs of batch latexes: (A) P(St–NIPAM) without AEM (DD1A); (B) P(St–NIPAM) with AEM (DD2)

rate is enhanced (see Fig. 1); in that case, at 20% conversion, NIPAM is almost totally consumed. The nucleation mechanism probably involves a shorter coagulation step due to the electrostatic stability imparted by the cationic groups brought by AEM, therefore a much larger number of particles is created. The obtained low particle size means that a particle number roughly one order of magnitude higher than without AEM is produced, however, the overall polymerization rate is only slightly larger than with only NIPAM. Two effects may be suggested for explaining such a behavior: (i) a decrease of the capture rate coefficient of the water-initiated charged radicals by the growing particles due to the presence of an electrosteric layer around the particles as recently shown by Gilbert [22] (ii) the transfer reaction entailed by the presence of AEM may also contribute to play a role by enhancing the termination event in the aqueous phase. Both effects can predominantly contribute to the formation of larger amounts of water-soluble polymers than in the AEM-free experiments. As observed in SEM micrographs (Fig. 8), the particle shape seems to reveal an uneven structure somewhat different from that observed in the AEM-free latexes. This could reflect the discrepancies imparted by AEM in the coagulative nucleation process leading to mature particles.

Concerning the shot latexes, the large differences observed in the particle morphology according to the conversion of the seed at which the monomer addition was carried out, also deserve some tentative explanation. It was clear that raspberry-like structure occurred when the shot monomer addition was performed early in the conversion of the polystyrene-rich core, whereas the particles became smoother as this addition took place at higher yield. The following mechanism may be suggested:

(i) At low or intermediate conversion (30–50%), most of the styrene monomer has diffused into the growing particles, so when adding the NIPAM–MBA–AEM mixture, a part of NIPAM (and possibly the cross-linker MBA) could be also partitioned in the styrene-swollen poly[NIPAM]-rich particles. Partition experiments, indeed, showed that almost 40 mol% of NIPAM can be solubilized in the styrene phase. Water-phase polymerization of both the hydrophilic and cationic monomers first occurs, providing charged poly[NIPAM]-rich macroradicals which can be captured by the particles, according to their hydrophobicity above the LCST and their concentration. Polymerization continues by propagation of the radicals into the monomer swollen particles. Because of the styrene-rich composition and favorable set of reactivity ratios ($r_s = 1.2$–1.4 and r_A (acrylamide derivatives) = 0.3–0.6 [20]), styrene-rich copolymer phase is growing in the outer layer of the particle but, due to a poor compatibility with the already formed polymer, this copolymer can rapidly phase separate as spherical occlusions containing polystyrene-rich modules. In addition, the anchoring effect of the cationic initiator fragments may prevent further diffusion of these polystyrene-rich domains into the particle, explaining that they are not far from the surface. This process of phase demixing could be significantly enhanced due to the presence of the cross linker in the shot addition (MBA). However, according to QELS size data which show the presence of a thermosensitive hydrophilic shell layer, it is obvious that most of the polymerized NIPAM is located at the particle surface.

(ii) At higher conversion the phase separation would be restricted due to the viscosity increase within the polymer particles. In addition, since the amount of the remaining styrene in the particles is smaller, the composition of the formed copolymers is richer in NIPAM, than forming a shell containing a more polar material. At very high conversion, mostly cross-linked NIPAM–AEM copolymer chains are produced, covering the particle core by a smooth shell, as it was found in the case of pure cationic poly[NIPAM] latexes [23].

In conclusion, all these cationic styrene–NIPAM copolymer particles exhibit a complex core-shell structure, the morphology, composition and thickness of the outer layer being determined both by the polymerization process and the concentration of the cationic monomer (AEM). Before using these latex particles as supports for biomolecules, a careful characterization of the surface and colloidal properties has been completed together with the consequences on the electrophoretic mobility and colloidal stability as a function of pH, ionic strength and temperature. It will be published as a second part of this series.

Acknowledgements The authors gratefully acknowledge Prof. H. Kawaguchi (Keio University Japan) for fruitful discussions and suggestions.

References

1. Yoshioka H, Mikami M, Nakai T, Mori Y (1994) Polym Adv Tech 6:418–420
2. Kawaguchi H, Fujimoto K, Mizuhara Y (1992) Colloid Polym Sci 270:53–57
3. Pelton RH, Chibante P (1986) Colloids Surf 20:247–257
4. Snowden MJ, Marston NJ, Vincent B (1994) Colloid Polym Sci 272: 1273–1280
5. Makino K, Yamamoto S, Fujimoto K, Kawaguchi H, Ohshima H (1994) J Colloid Interface Sci 166:251–258
6. Pelton RH (1988) J Polym Sci: Part A: Polym Chem 26:9–18
7. Fujimoto K, Mizuhara Y, Tamura N, Kawaguchi H (1996) J Int Mat Syst Struct 4:184–189
8. Kondo A, Kaneko T, Higashitani K (1994) Biotech Bioeng 44:1–6
9. Hoshino F, Fujimoto T, Kawaguchi H, Ohtsuka Y (1987) Polym J 19:241–247
10. Hoshino F, Kawaguchi H, Ohtsuka Y (1987) Polym J 19:1157–1164
11. Kawaguchi H, Hoshino F, Ohtsuka K (1986) Makromol Chem Rapid Commun 7:10–114
12. Ohtsuka Y, Kawaguchi H, Sugi Y (1981) J Appl Polym Sci 26:1637–1647
13. Wu X, Pelton RH, Hamielec AE, Wood DR, McPhee W (1994) Colloid Polym Sci 272:467–477
14. Meunier F, Elaissari A, Pichot H (1995) Polym Adv Technol 6:489–496
15. Kawaguchi H, Sugi Y, Ohtsuka Y (1981) J Appl Polym Sci 26:1649–1657
16. Hoshino F, Fujimoto T, Kawaguchi H, Ohtsuka Y (1987) Polym J 19:241–247
17. Zhang J, Pelton R, Deng Y (1994) Langmuir 11:2301–2302
18. Pelton RH, Pelton HM, Morfesis A, Rowell RL (1989) Langmuir 5:816–818
19. Park TG, Hoffman AS (1994) Polym J 52:85–89
20. Ganachaud F, Sauzedde F, Elaissari A, Pichot C (1997) J Appl Polym Sci 65:2315–2330
21. Greenley RZ (1989) In: Brandrup J and Immergut EH (eds) Polymer Handbook. Wiley Interscience, New York, p II-155
22. Gilbert RG (1997) In: Asua J (ed) Polymeric Dispersions: Principles and Applications. NATO ASI Series, Kluwer Academic Press, Dordrecht, p 1
23. Meunier F (1996) PhD Thesis, University of Lyon I